



Sharif, A., Althobaiti, T., Alotaibi, A.A., Ramzan, N., Imran, M.A. and Abbasi, Q.H. (2022) Inkjet-printed UHF RFID sticker for traceability and spoilage sensing of fruits. *IEEE Sensors Journal*, 23(1), pp. 733-740. (doi: 10.1109/JSEN.2022.3224811)

This is the Author Accepted Manuscript.

There may be differences between this version and the published version. You are advised to consult the publisher's version if you wish to cite from it.

<http://eprints.gla.ac.uk/286267/>

Deposited on: 08 December 2022

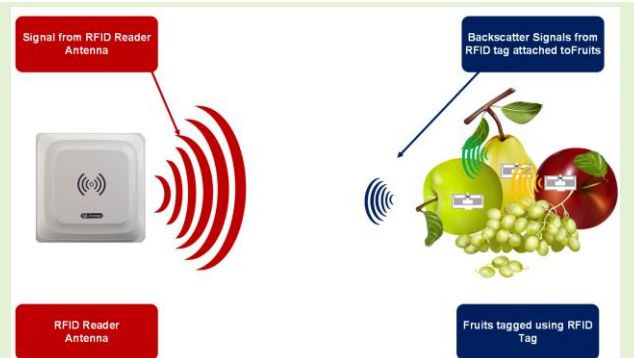
Enlighten – Research publications by members of the University of Glasgow
<http://eprints.gla.ac.uk>

Inkjet-printed UHF RFID Sticker for Traceability and Spoilage Sensing of Fruits

Abubakar Sharif, *Member, IEEE*, Turke Althobaiti, *Member, IEEE*, Abdullah Alhumaidi Alotaibi, *Member, IEEE*, Naeem Ramzan, *Senior Member, IEEE*, Muhammad Ali Imran, *Senior Member, IEEE* and Qammer H. Abbasi, *Senior Member, IEEE*

Abstract—This paper presents an ink-jet printed ultra-high frequency (UHF) radio frequency identification (RFID) label for tagging fruits. The proposed tag antenna is based on a hybrid configuration, which consists of a loop, dipole-like strips, and eye-shaped rectangular nested slots. The loop fulfills impedance matching purposes, while the eye-shaped slots assist to maintain high imaginary impedance to mitigate capacitive effects of high permittivity surfaces of fruits. Moreover, the dipole strips help to reduce the loss resistance caused by the high permittivity of the surface of the fruit. Therefore, the overall tag configuration provides a good impedance match with the Alien H3 RFID chip in the whole US UHF RFID band. Furthermore, the fabricated prototype of the proposed tag antenna achieved a read range of 3 m after mounting on Apple. Moreover, an automatic weighing and billing experiment is performed by placing the tagged apples inside a refrigerator. Overall, the performance of the proposed tag antenna is tested after mounting on apple fruits of different shapes and sizes which indicates the robustness of this tag. Moreover, the tag antenna is also tested for sensing spoilage of apple fruits. The read range of the proposed tag antenna reduces up to 42 % on spoiled apples. Therefore, this tag can be suitable for automatic sorting, weighing, and billing of fruits in smart cities, vending machines, and departmental stores.

Index Terms— Internet of Things (IoT), passive RFID (Radio Frequency Identification), Spoilage sensing, UHF (Ultra High Frequency) RFID tags



I. INTRODUCTION

RFID and IoT have been emerging day to day in numerous application areas ranging from the supply chain, sensing, tracking, healthcare, and so forth. UHF RFID is one of the key enabler technology of the IoT family [1]–[3]. For decades, fruits and vegetables have been an important element of the human diet. People in the present era are more interested in natural and organic nutrition because of the rise in disease variants. Fruits and vegetable contaminated with microorganisms may result in serious health issues.

Corresponding author: Qammer H. Abbasi)

Abubakar Sharif is also with Department of Electrical Engineering and Technology, Government College University Faisalabad. (email: sharifuftc@gmail.com)

Turke Althobaiti is with Department of computer science, Faculty of Science, Northern Border University, Arar, Saudi Arabia.

Turke Althobaiti is also with Remote Sensing Unit, Northern Border University, Arar, Saudi Arabia; Turke.althobaiti@nbu.edu.sa.

Abdullah Alhumaidi Alotaibi is with Department of Science and Technology, College of Ranyah, Taif University, P.O. Box 11099, Saudi Arabia. a.alhumaidi@tu.edu.sa.

Naeem Ramzan is with School of Computing, Engineering and Physical Sciences, University of the West of Scotland, Paisley PA12BE, UK; naeem.ramzan@uws.ac.uk.

Abubakar Sharif, Muhammad Ali Imran and Qammer H. Abbasi are with James Watt School of Engineering, University of Glasgow, Glasgow G12 8QQ, U.K. (e-mail: muhammad.imran@glasgow.ac.uk; qammer.abbasi@glasgow.ac.uk).

Decomposed fruits and vegetables cause various issues for food-related companies and marketplaces during imports and exports, as well as storage [4],[5]. So, a traceability and spoilage sensing system is required for fruits to prevent food wastage. The significance of UHF RFID systems lies in their longer reading distances and low-cost, inkjet-printable tags. However, the UHF tags are sensitive to background tagging surfaces and objects [6-11]. More precisely, the performance parameters of UHF tags such as impedance matching with RFID chips and radiation characteristics severely deteriorated on high permittivity materials and metallic surfaces. There were several techniques have been reported in the literature to mitigate such effects and improve the performance of UHF tags. However, most of these tags and techniques were based on thick substrates, which makes the UHF tags bulky and costly for most applications [12]. A folded dipole antenna based on a single layer of Polytetrafluoroethylene (PTFE) has been proposed in [13]. It is composed of C-shaped resonators and dipole arms embedded with outer strips for size reduction. The tag antenna has a size of $82.75 \times 19.5 \times 1.5 \text{ mm}^3$. However, this tag design is costly and has a large size from a mass production perspective. A spiral resonator-based S-shaped folded dipole tag with dual-band features has been presented in [14]. Although, this tag design posed a relatively small dimension, however, this tag design has a small read

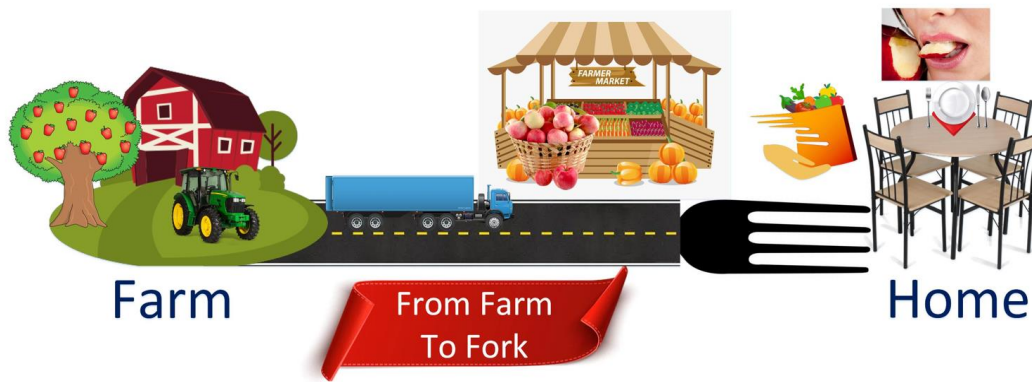


Fig. 1. The sustainable food system and food security perspectives such as the concept of farm to folk.

range along with a costly structure as compared to printed tags. An optically transparent flexible RFID tag antenna with circular polarization features was proposed. The tag design is based on a planner circular ring and the whole tag configuration is encapsulated inside transparent polymer. The transparent tag achieved a read range of 8.3 m [15]. A flexible tag antenna with a relatively long read range has been designed in [16] using graphene-based film. The graphene film is embedded in a polyethylene terephthalate (PET) substrate. This tag achieved a read range of 14 m. In [17], a flexible UHF RFID tag is designed for sensor applications. The tag antenna was comprised of a semicircular feed configuration and a meander line radiator. This tag antenna is fabricated on photo paper using silver nanoparticle ink. This tag has a size of $44 \times 59 \times 0.54 \text{ mm}^3$. Another inkjet-printed tag has been proposed for sensing salinity and sugar contents of water. This tag design consists of a slot-match technique that provides a good imaginary impedance above high permittivity surfaces. The slot-match tag has a size of $64.5 \times 15 \text{ mm}^2$ [18]. In [19], a folded dipole and loop matching-based design was devised for liquid-filled bottles. Although, this tag design achieved a read range of 4.2 m after mounting on water bottles. The dimensions of the bottle tag are $80 \text{ mm} \times 24 \text{ mm}$, however, its size is large for tagging fruits.

A washable UHF RFID passive tag-based sensor was devised in [20] for the moisture sensor of the diaper. The sensor design achieved on body read range of 3.6 m and 4.4 m on a baby diaper and adult diaper, respectively. The reader system is attached to the internet for generating an alert for parents or caregivers regarding the presence of moisture. The size of the tag design is $105 \times 06 \text{ mm}^2$. A flexible UHF RFID has been proposed for ice sensing [21]. Despite other techniques, this paper exploits to increase the read range of tag antenna for ice superstrate cases. This sensor tag has a read range of 9.4 m and 10 m in unloaded and ice-loaded scenarios as the superstrate. The tag antenna is encapsulated in Kapton and has dimensions of $109 \times 3.5 \text{ mm}^2$.

A complementary split-ring resonator (CSRR) based circularly polarized sensor tag design has been proposed for detecting the complex permittivity of liquids. The liquid under test was injected into the cavity through a hole. The complex permittivity of liquids was extracted by manipulating the

measure read range [22]. Similarly, a passive wire-less label type tag antenna was proposed for sensing the dielectric properties of aqueous liquids. An unobtrusive, safe monitoring solution was proposed by attaching a label antenna to a Petri plate or clear borosilicate glass bottle. The proposed tag was based on a parasitic matching loop and half-wave dipole antenna with a 29 mm diameter [23].

Most of the aforementioned substrate-based tag designs were too bulky or costly for tagging fruits. Moreover, the inkjet-printed/inlay-type tags devised for water bottles also have large dimensions. Therefore, this paper presents a low-cost flexible UHF RFID tag design for tagging fruits. The tag is based on loop match, eye-shaped slots, and dipole-like strips to provide a good impedance match over the surface of Apple. This tag configuration provides a good match with an impedance of the Alien H3 RFID chip in the whole US UHF RFID band. Moreover, the tag antenna achieved a read range of 3 m after mounting on Apple. Additionally, an automatic billing experiment is performed by placing the tagged apples inside a refrigerator. The performance of the proposed tag antenna is verified after mounting on apple fruits of different shapes and sizes. Therefore, this tag can be suitable for automatic sorting, weighting, and billing of fruits in smart cities, and further assists sustainable food system and food security perspectives such as the concept of farm to folk [24] or farm to home as described in Fig. 1.

II. TAG ANTENNA CONCEPT AND DESIGN

Fig. 2 illustrates the detailed dimensions and configuration of the proposed RFID tag design.

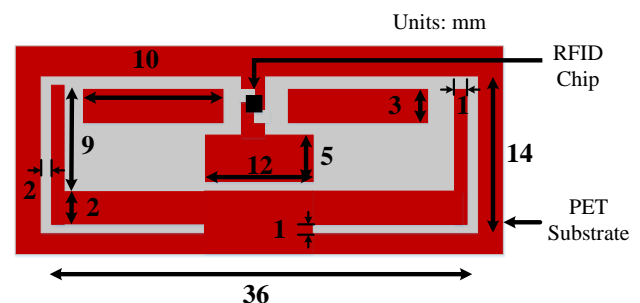


Fig. 2. Detailed dimensions and configuration of proposed RFID tag design.

This tag design is fabricated on a 0.2 mm PET substrate. The hybrid tag structure exploits the features of eye-shaped nested slots (ENS) and the loop matching technique (LMT) [25]. The combination of ENS and LMT offers a good imaginary impedance match with the RFID chip. The LMT counters the capacitive impedance of the RFID chip, while ENS assists to counter the capacitive effects of high permittivity surfaces such as Fruits. Thanks to the inductive reactance of ENS configuration that can offer a good imaginary impedance match, especially on high permittivity dielectrics. To investigate it further, a two-layered apple model (as depicted in Fig. 3) is simulated in CST Microwave Studio (MWS). The electrical properties of the apple were listed in [26], [27] states that external issues of the apple have permittivity ranging from 20 – 24 (at 915 MHz), while internal tissue has permittivity ranging from 67 – 74 (at 915 MHz).

The effects of the challenging surface of fruits such as apples were studied and analyzed by mounting the tag antenna on these surfaces. The tag structure is translated into an equivalent circuit (EC) according to the formulations reported in [28] – [30] as shown in Fig. 4 (a). It is observed that the high permittivity of apples causes an increase in loss resistance. The effects of apple on tag performance are mitigated by modifying the equivalent circuit of tags.

Furthermore, by analyzing the full-wave simulated results obtained from CST, the equivalent circuit is simulated using ADS software. The optimized values of equivalent circuits are achieved by fine-tuning in ADS and curve fitting in Matlab, respectively. The increase in loss resistance is compensated by adding an equivalent RLC circuit in parallel to the main tag EC. The modified EC with parallel RLC is shown in Fig. 4(b). Finally, the modified equivalent circuit is translated back to the modified tag structure, which resulted in the shape of dipole-like strips. More precisely, the increase in loss resistance due to the fruit surface is compensated by adding a dipole-like strips as shown in Figure 4 (c). The tag parameters are optimized further using CST Microwave studio to get a conjugate match with the Alien H3 RFID chip with impedance 28-201j at 915 MHz.

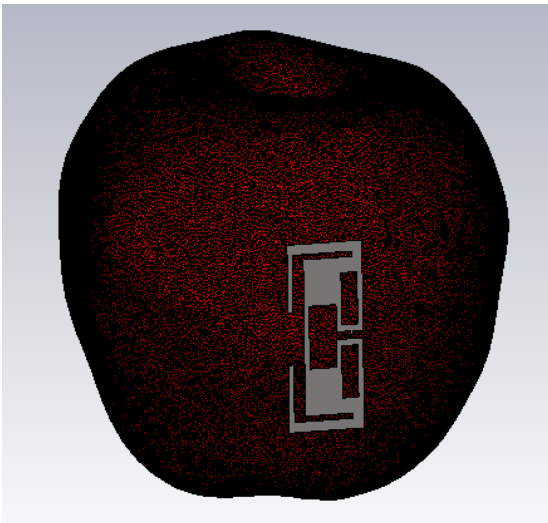


Fig. 3. Two-layered apple model simulated in CST MWS along with RFID tag design.

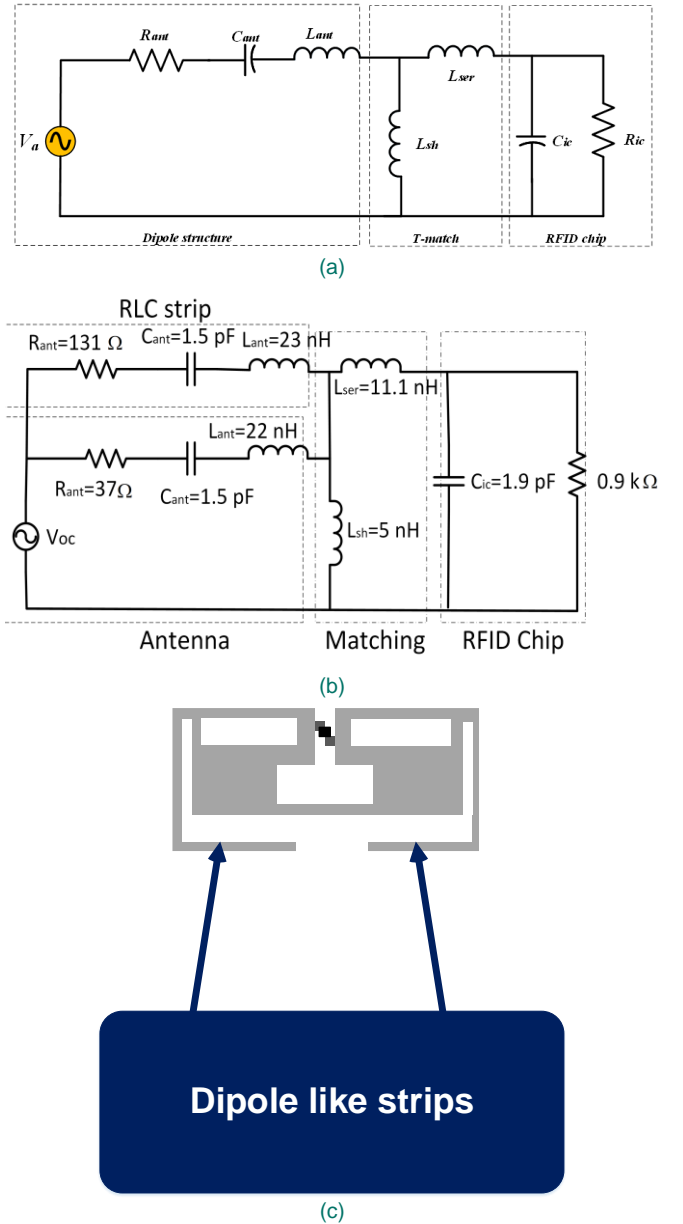


Fig. 4. (a) Equivalent Circuit (EC) of RFID tag antenna (b) Modified Equivalent Circuit model of pro-posed tag to compensate the increase in loss resistance. (c) Dipole strips resulted after modifying EC

III. SIMULATION RESULTS AND MEASUREMENTS

A. Impedance Match and Reflection Coefficient

Fig. 5 illustrates the impedance plot of the first variant and proposed tag after mounting on a flat apple surface. The introduction of dipole-like strips (DLS) in the first variant of the apple tag compensated the increased loss resistance due to the high permittivity of the apple. The first variant provides an imaginary impedance of 150 Ω to 160 Ω in the US UHF RFID band (902 MHz - 928 MHz). While the real impedance ranges from 25 Ω to 35 Ω , that matches well with the H3 chip. However, the imaginary impedance of the H3 RFID chip ranges from 180 Ω to 190 Ω in the US RFID band.

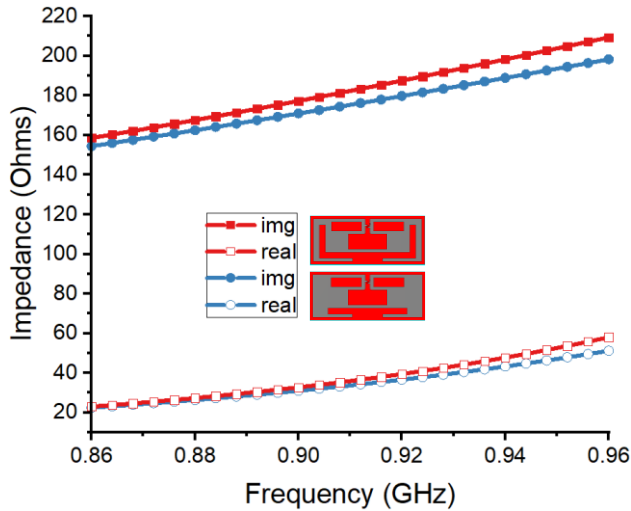


Fig. 5. Real and imaginary impedance plot of first variants and proposed tag after mounting on flat apple surface.

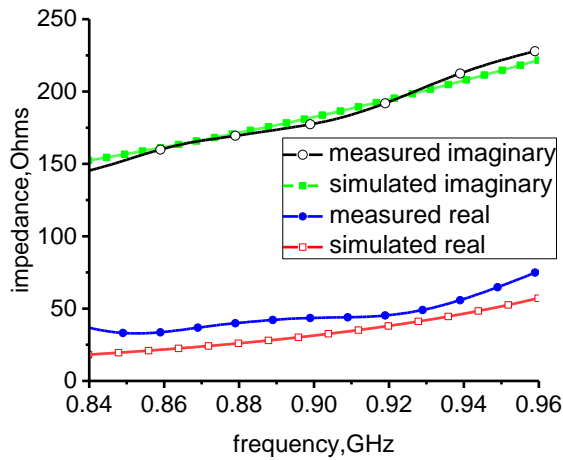


Fig. 6. Real and imaginary impedance plot of proposed apple tag after mounting on Curved apple surface (less than 15°).

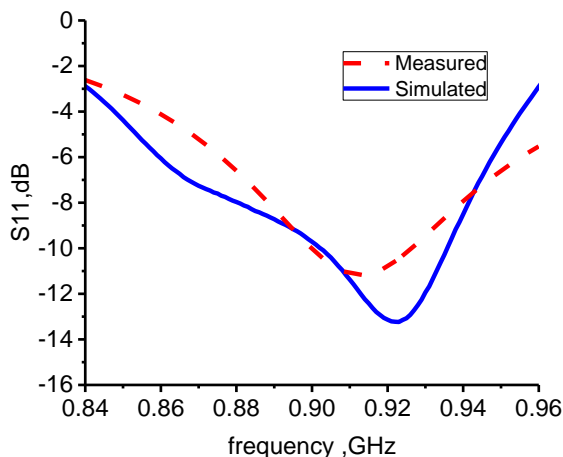


Fig. 7. S11 parameter plot of proposed apple tag after mounting on Curved apple surface (less than 15°).

Therefore, the slots are added across the strips to match the imaginary impedance of the apple tag with H3. The slots increase the imaginary impedance without any significant change in the real impedance of the apple tag design. Moreover, the previous simulated real and imaginary impedances of apple tags are estimated by considering a flat apple surface model.

Fig. 6 illustrates the simulated as well as measured results regarding the impedance of the apple tag after mounting on a curved apple surface. The imaginary and real impedance do not change much as long as the conformal angle/surface is less than 15° . However, the results deteriorate significantly after the curve angle increased more than 30° . As it can be seen from Fig. 6, the measured real and imaginary impedances of the apple tag match well with each other and the H3 RFID chip. However, there is a slight increase in the value of measured real impedance as compared to the simulated one. The measured real impedance has a value of around $40 - 50 \Omega$ recorded after testing on 10 different apples. To measure impedance, a probe formed by connecting the outer coax of two coaxial cables (also known as balance-to-unbalance (balloon) probe) is employed with an Agilent vector network analyzer (Agilent E8363B) and MATLAB code. The tag inlay without a chip is used for impedance measurement.

Similarly, the corresponding simulated and measured results S11 parameter plot of apple tag after placing on apples is shown in Fig. 7. There is a little discrepancy in the value of the measured S11 parameter with the simulated one, which is due to the increased value of the measured real impedance value. Finally, the measured impedance and corresponding S11 match well with the simulated one.

To elaborate it further, the impedance performance of proposed tag design for more than 15° curved or bending surface are also discussed. The real and imaginary impedance of proposed apple tag along with S11 parameter for more than 15° is depicted in Fig. 8. Although, the performance of this tag design is getting worsen even at 16° . However, the impedance and S11 performance of apple tag shown in Fig 8 are taken at 20° curved or bending surface.

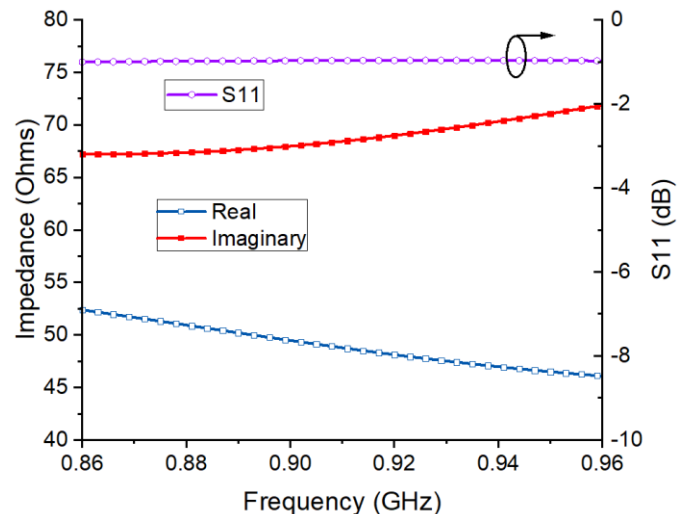


Fig. 8. Real and imaginary impedance and S11 plot of proposed apple tag after mounting on Curved apple surface (more than 15°).

B. Read range Measurement and Setup

Finally, the read range of tagged apples has been tested to verify the performance of the apple tag. For the read range measurement proposes, the fabricated tag with an H3 RFID chip is mounted on apples as shown in Fig. 9. The read range is measured using two different setups 1) Tagformance Pro unit and 2) Impinj R420 UHF RFID reader with a circularly polarized antenna. The read range of the proposed tag obtained using the Tagformance Pro setup ranges from 4.5 m to 5.5 m using a linearly polarized reader antenna. Fig. 10 shows the Tagformance Pro setup for the read range measurements of the apple tag. A foam spacer was placed between the tagged apple and the linear polarized antenna.



Fig. 9. Fabricated prototype of apple tag on two different apple samples.

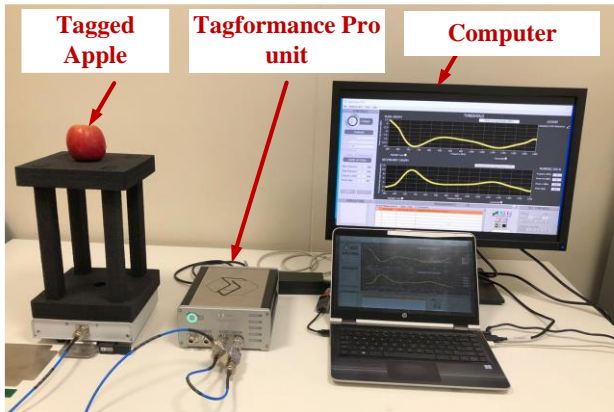


Fig. 10. Tagformance Pro setup for read range and RSSI measurement of tag after mounting on apples.

To investigate it further, the read range of the apple tag has been recorded in an indoor lab environment using an IMPINJ R420 RFID reader and circularly polarized antenna as depicted in Fig. 11. The EIRP (Effective Isotropic Radiated Power) of the reader was set to 4W for reading range testing. Moreover, the read range testing is done by using apples of different shapes and sizes. The read range of two apples after mounting on curved apple surfaces is shown in Fig. 11. The apple 1 has approximately 5° and the apple 2 has 15° curved surface. The read range is tested for almost 10 apples. Almost, all apple samples give similar read ranges in the US RFID band. The maximum read range recorded using this setup is 3.2 m. To prove the robustness of the apple tag, the read range was recorded from different directions by pasting the tag

both horizontally and vertically (as listed in Table I). The maximum read range achieved from the direction is almost 3 m for both horizontally and vertically tagged apples. The read range from back size is recorded as almost 2 m for both aforementioned cases. Additionally, the read range is also recorded from a downwards direction after placing the apple on foam above the RFID reader antenna. The read distance with a downwards direction is recorded to be 2.5 m and 2.9 m for apple 1 and apple 2, respectively. Therefore, this proposed apple tag achieved a read distance of about 2 m in all directions.

TABLE I
READ RANGE OF APPLE TAG IN DIFFERENT DIRECTIONS

Apple samples	Measured read range from different directions		
	Front (m)	Back (m)	Downward (m)
Apple 1 with horizontal tag	2.9	2	2.5
Apple 2 with horizontal tag	3	2.1	2.9
Apple 1 with vertical tag	3.1	2.1	2.5
Apple 2 with vertical tag	3.2	2.5	2.9

C. Spoilage Sensing Experiment

The spoilage of apples can be sensed by detecting the reduction in reading range or RSSI (received signal strength indicator). The changes in permittivity of the apple's upper or inner surface cause a mismatch between the impedance of the RFID chip and the tag. Moreover, if spoilage results in watering the inner surface, there will be also gain reduction, which also results in read range reduction.

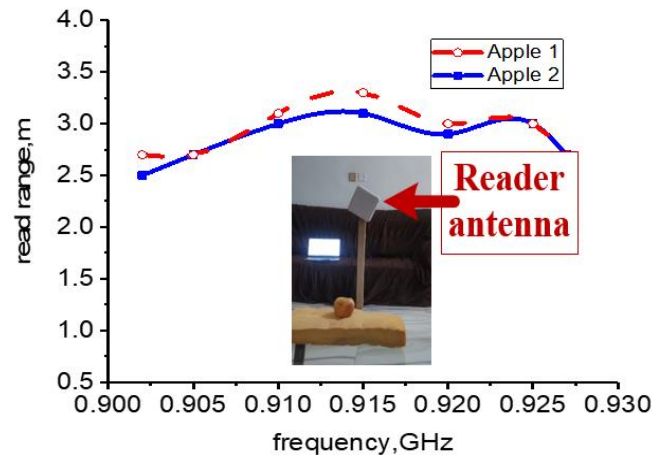


Fig. 11. Measured read range of apple tag after mounting on apples using reader and circular polarized antenna.

The RSSI can be estimated using the method presented in [31]. Moreover, the RSSI can be recorded either using an RFID reader setup or Tagformance Pro setup. Considering, the known reader parameters such as reader antenna gain G_{Reader} , input power P_t and d is the distance between the RFID reader and tagged substance. Let ϑ is the change in permittivity of apple surface due to spoilage.

$$P_r = \frac{P_t G_{Reader}}{4\pi d^2} * \frac{\lambda^2}{4\pi} G_{Tag}[\vartheta] \eta_p \quad (1)$$

Where $G_{Tag}[\vartheta]$ is gain of the tag and η_p is polarization mismatch between reader antenna and tag.

$$|\Gamma_m(\vartheta)| = \frac{Z_{chip} - Z_{Tag}[\vartheta]}{Z_{chip} + Z_{Tag}[\vartheta]} \quad (2)$$

Where $|\Gamma_m(\vartheta)|$, $Z_{chip} = R_{chip} + jX_{chip}$ and $Z_{Tag}[\vartheta] = R_{Tag}[\vartheta] + jX_{Tag}[\vartheta]$ are reflection coefficient, RFID chip impedance and Tag impedance resulted due to change in permittivity of the background surface.

$$\tau[\vartheta] = \frac{4R_{chip}R_{Tag}[\vartheta]}{|Z_{chip} + Z_{Tag}[\vartheta]|^2} \quad (3)$$

The $\tau[\vartheta]$ represents the corresponding power transmission coefficient with respect to the change in permittivity.

Finally, the RSSI can be estimated as follows

$$P_{RSSI}[\vartheta] = \frac{1}{4\pi} \left(\frac{\lambda}{4\pi d} \right)^2 P_t G_{Reader}^2 r_{CS_T}[\vartheta] \eta_p^2 \quad (4)$$

Where $r_{CS_T}[\vartheta]$ is the RFID tag's radar cross-section.

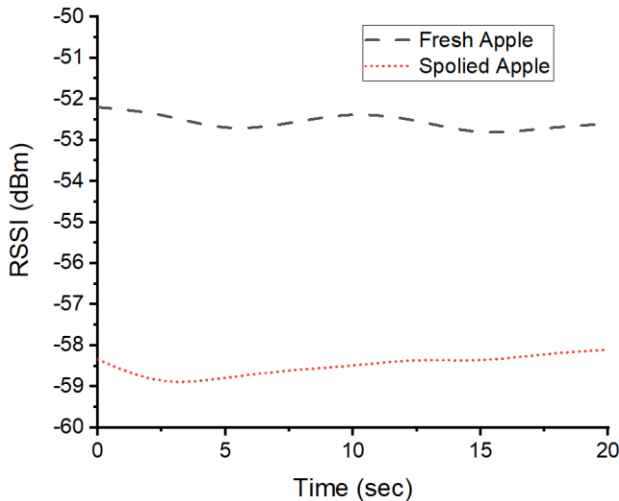


Fig. 12. Measured RSSI vs time for fresh and spoiled apples in laboratory environment.

$$r_{CS_T}[\vartheta] = \frac{\lambda^2}{4\pi} G_{Tag}^2[\vartheta] \bullet |\Gamma_m(\vartheta)|^2 \quad (5)$$

The change in permittivity of the apple is estimated using the corresponding RSSI $P_{RSSI}[\vartheta]$.

The Tagformance-based setup is used to record the RSSI value of fresh and spoiled apples in a laboratory environment as shown in Fig. 9. The same set of apples was used to record the RSSI in the spoiled case after placing the fresh apples outside the refrigerator for one week. It can be seen from Fig. 12, that the RSSI of the tag antenna mounted on fresh apples is approximately -52 dBm, while the RSSI on spoiled apples is recorded as -58 dBm. Therefore, there is a decrease in RSSI value by about 6 dB for spoiled apples. The reduction in RSSI value is due to the difference in the dielectric constant of apples during the spoilage process. We have tested almost 10 different apples for spoilage testing. Fig. 13 shows a sample of spoiled apples with and without the proposed apple tag. There is approximately a 42 % decrease in the read range of the proposed tag on spoiled apples. Therefore, the proposed apple tag can successfully detect the spoilage of apples.



Fig. 13. Spoiled apple sample with or without mounting proposed apple tag.

D. Automatic Billing Experiment

An application of the proposed apple tag is also devised by placing it inside a refrigerator for an automatic billing experiment. A similar experiment proposed in [3] is repeated for the automatic billing of apples. The experimental setups are depicted in Figs. 14 and 15. As illustrated in Fig. 14, two apple samples were placed in a refrigerator along with a circularly polarized reader antenna installed at the bottom of the refrigerator. The RFID tags were affixed horizontally and vertically on apple samples. The reader successfully reads both tagged apples placed in different orientations.

The QR code pasted on the refrigerator door is scanned using an online payment application such as WeChat or Alipay. The door of the refrigerator is opened after confirming the account balance payment application server. The user can pick any tagged apple. The reader antennas are mounted beneath each shelf as shown in Fig. 15. The reader antennas assist RFID reader to count the picked tags after door of refrigerator is closed. The picked tagged apples are automatically billed from customer payment account after the door of the refrigerator is closed.

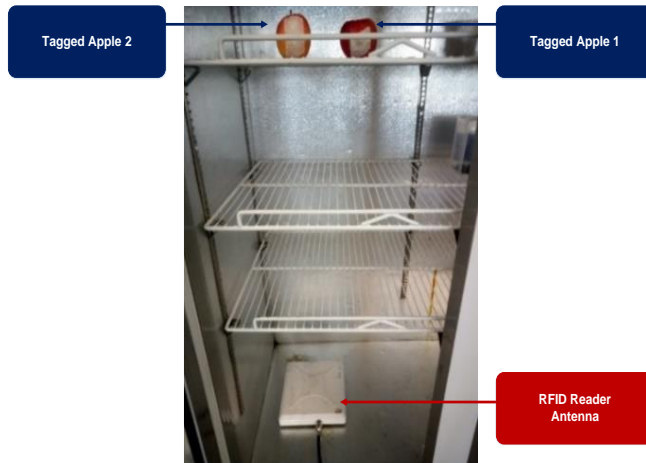


Fig. 13. Tagged apple samples are placed in refrigerator for automatic billing experiment.

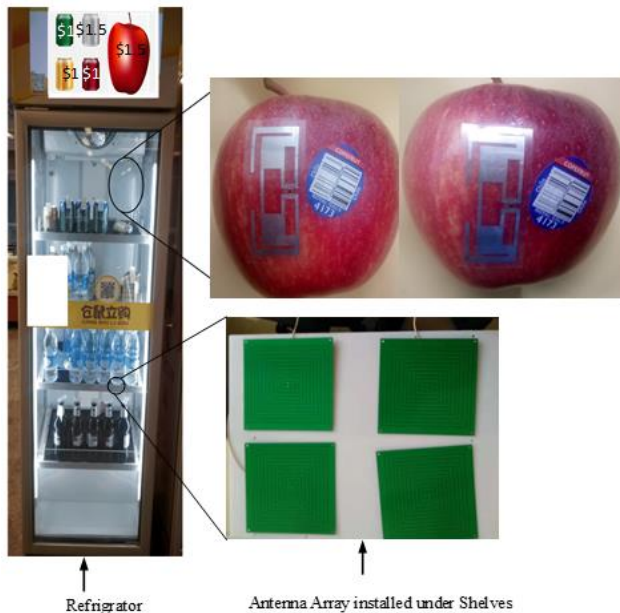


Fig. 14. Refrigerator system based on UHF RFID technology for automatic billing of beverage and fruits.

IV. CONCLUSION

A low-cost inkjet printed label was proposed for tagging and spoilage sensing of fruits such as apples. The tag was based on eye-shaped slots, matching loop, and dipole-like strips to counter the effects of the high permittivity of the surface of the fruit. The proposed tag configuration provides a good impedance match with the Alien H3 RFID chip in the US RFID band. Moreover, the apple tag also achieved a read range of 3 m after pasting on apples. Additionally, an automatic billing experiment is performed by placing the tagged apples inside a refrigerator. Overall, to prove the robustness of the proposed solution, the performance of the proposed tag antenna was tested after mounting on apple fruits of different shapes and sizes. Moreover, the tag antenna was also tested for sensing

spoilage of apple fruits. There was approximately a 6 dB difference recorded in RSSI value for tags pasted on fresh and spoiled apples. Accordingly, the read range of the proposed tag antenna reduces up to 42 % on spoiled apples. Therefore, this tag can be suitable for automatic sorting, weighting, and billing of fruits in smart cities, vending machines, and departmental stores. For future work, this spoilage sensing approach can be further combined with machine learning and other sensing techniques such as relative humidity, temperature, and carbon dioxide to develop digital twins in order to predict freshness.

ACKNOWLEDGMENT

The authors extend their appreciation to the Deputyship for Research & Innovation, Ministry of Education in Saudi Arabia for funding this research work through the project number (IF_2020_NBU_333).

REFERENCES

- [1] S. Kim, Y. Kawahara, A. Georgiadis, A. Collado, and M. M. Tentzeris, "Low-cost inkjet-printed fully passive RFID tags for calibration-free capacitive/haptic sensor applications," *IEEE Sens. J.*, vol. 15, no. 6, pp. 3135–3145, 2015, doi: 10.1109/JSEN.2014.2366915.
- [2] C. Savaglio and G. Fortino, "A Simulation-driven Methodology for IoT Data Mining Based on Edge Computing," *ACM Trans. Internet Technol.*, vol. 21, no. 2, Mar. 2021, doi: 10.1145/3402444.
- [3] S. Gopikrishnan, P. Priakanth, G. Srivastava, and G. Fortino, "EWPS: Emergency Data Communication in the Internet of Medical Things," *IEEE Internet Things J.*, vol. 8, no. 14, pp. 11345–11356, Jul. 2021, doi: 10.1109/JIOT.2021.3053419.
- [4] O. Kemiklioglu, Emine; Ozen, "Design of a Sensor to Detect Fruit Freshness," *Int. J. Sci. Technol. Res.*, vol. 4, no. 1, pp. 1–6, 2018, Accessed: Sep. 25, 2022. [Online]. Available: <https://www.iiste.org/Journals/index.php/JSTR/article/view/40898>.
- [5] N. M. Shaalan, F. Ahmed, S. Kumar, A. Melaibari, P. M. Z. Hasan, and A. Aljaafari, "Monitoring Food Spoilage Based on a Defect-Induced Multiwall Carbon Nanotube Sensor at Room Temperature: Preventing Food Waste," *ACS Omega*, vol. 5, no. 47, pp. 30531–30537, Dec. 2020, doi: 10.1021/acsomega.0c04396.
- [6] E. Perret, S. Tedjini, and R. S. Nair, "Design of antennas for UHF RFID tags," *Proc. IEEE*, vol. 100, no. 7, pp. 2330–2340, 2012, doi: 10.1109/JPROC.2012.2186950.
- [7] A. Sharif et al., "Low-cost inkjet-printed UHF RFID tag-based system for internet of things applications using characteristic modes," *IEEE Internet Things J.*, vol. 6, no. 2, pp. 3962–3975, Apr. 2019, doi: 10.1109/JIOT.2019.2893677.
- [8] R. Abdulghafor et al., "Recent Advances in Passive UHF-RFID Tag Antenna Design for Improved Read Range in Product Packaging Applications: A Comprehensive Review," *IEEE Access*, vol. 9, pp. 63611–63635, 2021, doi: 10.1109/ACCESS.2021.3074339.
- [9] C. Occhiuzzi et al., "Radio-frequency-identification-based intelligent packaging: Electromagnetic classification of tropical fruit ripening," *IEEE Antennas Propag. Mag.*, vol. 62, no. 5, pp. 64–75, Oct. 2020, doi: 10.1109/MAP.2020.3003212.
- [10] G. Fortino, C. Savaglio, G. Spezzano, and M. Zhou, "Internet of Things as System of Systems: A Review of Methodologies, Frameworks, Platforms, and Tools," *IEEE Trans. Syst. Man, Cybern. Syst.*, vol. 51, no. 1, pp. 223–236, Jan. 2021, doi: 10.1109/TSMC.2020.3042898.
- [11] W. Dong, L. Yang, R. Gravina, and G. Fortino, "Soft wrist-worn multi-functional sensor array for real-time hand gesture recognition," *IEEE Sens. J.*, vol. 22, no. 18, pp. 17505–17514, 2022, doi: 10.1109/JSEN.2021.3050175.
- [12] F. Costa, S. Genovesi, M. Borgese, A. Michel, F. A. Dicandia, and G. Manara, "A review of rfid sensors, the new frontier of internet of things," *Sensors*, vol. 21, no. 9, 2021, doi: 10.3390/s21093138.
- [13] F. Erman et al., "Miniature compact folded dipole for metal

- mountable UHF RFID tag antenna,” *Electron.*, vol. 8, no. 6, p. 713, Jun. 2019, doi: 10.3390/electronics8060713.
- [14] B. Barman, S. Bhaskar, and A. K. Singh, “Spiral resonator loaded S-shaped folded dipole dual band UHF RFID tag antenna,” *Microw. Opt. Technol. Lett.*, vol. 61, no. 3, pp. 720–726, Mar. 2019, doi: 10.1002/MOP.31647.
- [15] A. S. M. Sayem et al., “Optically Transparent Flexible Robust Circularly Polarized Antenna for UHF RFID Tags,” *IEEE Antennas Wirel. Propag. Lett.*, vol. 19, no. 12, pp. 2334–2338, Dec. 2020, doi: 10.1109/LAWP.2020.3032687.
- [16] B. Zhang, X. Tang, J. Zhang, C. Liu, D. He, and Z. P. Wu, “Long read range and flexible UHF RFID tag antenna made of high conductivity graphene-based film,” *Int. J. RF Microw. Comput. Eng.*, vol. 30, no. 1, p. e21993, Jan. 2020, doi: 10.1002/MMCE.21993.
- [17] M. T. Islam, T. Alam, I. Yahya, and M. Cho, “Flexible Radio-Frequency Identification (RFID) Tag Antenna for Sensor Applications,” *Sensors* 2018, Vol. 18, Page 4212, vol. 18, no. 12, p. 4212, Nov. 2018, doi: 10.3390/S18124212.
- [18] A. Sharif, J. Ouyang, A. Raza, M. A. Imran, and Q. H. Abbasi, “Inkjet-printed UHF RFID tag based system for salinity and sugar detection,” *Microw. Opt. Technol. Lett.*, vol. 61, no. 9, pp. 2161–2168, 2019, doi: 10.1002/mop.31863.
- [19] S. He, Y. Zhang, L. Li, Y. Lu, Y. Zhang, and H. Liu, “High performance UHF rfid tag antennas on liquid-filled bottles,” *Prog. Electromagn. Res.*, vol. 165, pp. 83–92, 2019, doi: 10.2528/pier19041001.
- [20] M. A. S. Tajin, W. M. Mongan, and K. R. Dandekar, “Passive RFID-Based Diaper Moisture Sensor,” *IEEE Sens. J.*, vol. 21, no. 2, pp. 1665–1674, Jan. 2021, doi: 10.1109/JSEN.2020.3021395.
- [21] M. Wagih and J. Shi, “Wireless Ice Detection and Monitoring Using Flexible UHF RFID Tags,” *IEEE Sens. J.*, vol. 21, no. 17, pp. 18715–18724, 2021, doi: 10.1109/JSEN.2021.3087326.
- [22] Y. Chen, C. Hua, and Z. Shen, “Circularly Polarized UHF RFID Tag Antenna for Wireless Sensing of Complex Permittivity of Liquids,” *IEEE Sens. J.*, vol. 21, no. 23, pp. 26746–26754, Dec. 2021, doi: 10.1109/JSEN.2021.3121714.
- [23] V. Makarovaite, A. J. R. Hillier, S. J. Holder, C. W. Gourlay, and J. C. Batchelor, “Passive Wireless UHF RFID Antenna Label for Sensing Dielectric Properties of Aqueous and Organic Liquids,” *IEEE Sens. J.*, vol. 19, no. 11, pp. 4299–4307, Jun. 2019, doi: 10.1109/JSEN.2019.2896481.
- [24] Europa Kommissionen, “Farm to Fork Strategy,” DG SANTE/Unit ‘Food Inf. Compos. food waste’, no. DG SANTE/Unit ‘Food Inf. Compos. food waste’, p. 23, 2020, Accessed: May 15, 2022. [Online]. Available: https://ec.europa.eu/food/horizontal-topics/farm-fork-strategy_en.
- [25] G. Marrocco, “The Art of UHF RFID Antenna Design: Impedance-Matching and Size-Reduction Techniques,” *IEEE Antennas Propag. Mag.*, vol. 50, no. 1, p. 14, 2008.
- [26] W. chuan Guo, S. O. Nelson, S. Trabelsi, and S. J. Kays, “10-1800-MHz dielectric properties of fresh apples during storage,” *J. Food Eng.*, vol. 83, no. 4, pp. 562–569, 2007, doi: 10.1016/j.jfoodeng.2007.04.009.
- [27] M. E. Sosa-Morales, L. Valerio-Junco, A. López-Malo, and H. S. García, “Dielectric properties of foods: Reported data in the 21st century and their potential applications,” *LWT - Food Sci. Technol.*, vol. 43, no. 8, pp. 1169–1179, 2010, doi: 10.1016/j.lwt.2010.03.017.
- [28] Dobkin, *The RF in RFID: Passive UHF RFID in Practice*. Elsevier Inc., 2007.
- [29] G. Zamora, S. Zuffanelli, F. Paredes, F. Martin, and J. Bonache, “Design and synthesis methodology for UHF-RFID tags based on the T-match network,” *IEEE Trans. Microw. Theory Tech.*, vol. 61, no. 12, pp. 4090–4098, 2013, doi: 10.1109/TMTT.2013.2287856.
- [30] D. D. Deavours, “Analysis and design of wideband passive UHF RFID tags using a circuit model,” in *2009 IEEE International Conference on RFID*, Apr. 2009, pp. 283–290, doi: 10.1109/RFID.2009.4911211.
- [31] C. Occhiuzzi, S. Caizzone, and G. Marrocco, “Passive UHF RFID antennas for sensing applications: Principles, methods, and classifications,” *IEEE Antennas Propag. Mag.*, vol. 55, no. 6, pp. 14–34, 2013, doi: 10.1109/MAP.2013.6781700.